Bulletin of Electrical Engineering and Informatics
Vol. 15, No. 6, December 2026, pp. 5068~5078
ISSN: 2302-9285, DOI: 10.11591/eei.v15i6.11689

Unified mobile framework for electrocardiogram-based myocardial infarction detection and arrhythmia classification

Sameer Ahmad Hasan, Samer Alabed, Talal Ayyoub, Abdullah Shahin
Department of Biomedical Engineering, School of Applied Medical Sciences, German Jordanian University, Amman, Jordan

Article Info

Article history:

Received Dec 21, 2025
Revised Sep 15, 2026
Accepted Oct 4, 2026

Keywords:

Electrocardiogram
Good health and well-being
Internet of things
Mobile health
Remote monitoring
Signal processing
Sustainable healthcare system

ABSTRACT

Cardiovascular diseases (CVDs), particularly myocardial infarction (MI) and arrhythmias, require timely and accurate computational support for screening and follow-up. This study presents a unified internet of things (IoT)-enabled electrocardiogram (ECG) framework for mobile MI detection and multiclass arrhythmia classification. The framework integrates ECG preprocessing using biorthogonal and median filtering, machine learning (ML)-based interpretation, and mobile application delivery for prompt diagnostic feedback. The main contribution of this work is the integration of MI detection and multiclass arrhythmia classification within a single mobile-health workflow. The best random forest (RF) model achieved 96.89% accuracy for MI detection. For arrhythmia classification, the selected RF model achieved 89.59% accuracy on the held-out test set. These findings support the potential of the proposed framework as a mobile decision-support system for ECG interpretation and remote follow-up. Because evaluation was performed on row-level samples rather than patient-disjoint data, the reported results should be interpreted as within-dataset decision-support performance. Overall, the framework provides a practical link between ECG interpretation and mobile-health delivery while supporting further validation in real-world deployment settings.

This is an open access article under the CC BY-SA license.

Corresponding Author:

Sameer Ahmad Hasan
Department of Biomedical Engineering, School of Applied Medical Sciences
German Jordanian University
Amman, 11180 Jordan
Email: sameer.hasan@gju.edu.jo

1. INTRODUCTION

Cardiovascular diseases (CVDs) are the leading cause of death globally. An estimated 17.9 million people died from CVDs in 2019, representing 32% of all global deaths, and 85% of these deaths were due to heart attack and stroke [1]. In Jordan, noncommunicable diseases (NCDs) account for nearly 80% of total deaths, with CVDs constituting 42% of all deaths [2]. Among patients with myocardial infarction (MI), arrhythmias are common and clinically important; one study reported arrhythmias in 89.1% of patients, of whom 64.5% had lethal arrhythmias [3]. These statistics highlight the need for timely and reliable automated detection of MI and arrhythmias. The heart, which consists of four chambers, two atria and two ventricles, functions as a dual-pump system, as shown in Figure 1. The right atrium and right ventricle circulate deoxygenated blood to the lungs, whereas the left atrium and left ventricle pump oxygenated blood to the body. Electrical impulses originating from the sinoatrial (SA) node regulate rhythmic cardiac contraction by coordinating atrial and ventricular activity [4].

The electrocardiogram (ECG) is a non-invasive diagnostic tool used to record the electrical activity of the heart. Standard 12-lead ECG recordings capture distinct phases of the cardiac cycle, as shown in

Figure 2, including the P wave (atrial depolarization), QRS complex (ventricular depolarization), and T wave (ventricular repolarization) [5], [6]. ECG analysis is essential for identifying conditions such as MI and arrhythmias. MI occurs when blood flow to part of the heart muscle is abruptly reduced or blocked, leading to ischemia and damage or death of myocardial cells [7]. Cardiac arrhythmias are abnormalities of heart rhythm caused by disturbances in the electrical impulses that coordinate heartbeats [8]. They may manifest tachycardia, bradycardia, or irregular rhythms such as atrial fibrillation (AFIB) and ventricular fibrillation, and may also include supraventricular tachycardia (SVTAC), ventricular tachycardia, and premature contractions [8], [9]. ECG interpretation may be supported by computational approaches such as wavelet-based signal analysis and Fourier-based decomposition [10], [11], as well as by complementary clinical tools such as echocardiography and biochemical markers including myoglobin, troponin, and creatine kinase [7]. In addition, recent machine learning (ML) and deep learning methods have improved ECG interpretation and enabled more targeted differentiation between MI and arrhythmic conditions [12]–[14].

Recent studies have reported strong performance in either MI detection or arrhythmia classification; however, direct comparison across studies remains difficult because datasets, label definitions, preprocessing strategies, lead configurations, and validation protocols vary substantially [12], [13], [15]–[17]. For example, Śmigiel *et al.* [16] reported accuracies of 89.2%, 76.5%, and 69.8% for 2-class, 5-class, and 20-class ECG classification on PTB-XL using a convolutional network with entropy features. Qu *et al.* [17] reported 94.11% accuracy, 94.97% sensitivity, and 90.98% specificity for MI detection on the PTB dataset using an interpretable shapelet-based deep model. Sattar *et al.* [18] reported 91.8% accuracy for cardiac arrhythmia classification using digitized ECG signals and highlighted the potential for real-time monitoring using a CNN-based model. In a wearable-oriented setting, Baca and Valdivia [19] reported 99.57% multiclass arrhythmia accuracy on MIT-BIH and demonstrated the feasibility of smartwatch deployment. Despite these advances, many studies focus on a single diagnostic task or emphasize offline model evaluation without showing how inference results are delivered within a practical mobile-health workflow [13], [17], [18], [20]. These gaps motivated this study, which proposes a unified internet of things (IoT)-enabled ECG framework that integrates signal preprocessing, ML-based interpretation, and mobile delivery for MI detection and multiclass arrhythmia classification.

The proposed system is intended to support timely ECG assessment, remote monitoring, and future wearable integration. However, clinical adoption depends not only on algorithmic performance, but also on safe triage support, usability, and deployment feasibility. In remote or resource-limited settings, IoT-enabled mobile ECG systems may improve access to early screening and follow-up by enabling automated interpretation and rapid feedback outside specialized centers. Nevertheless, false-positive and false-negative outputs, interface clarity, and interoperability with wearable ECG platforms remain important considerations. Accordingly, this framework provides a foundation for decision-support use in mobile ECG analysis and for further real-world validation toward deployment.

The main contribution of this work is the integration of ECG preprocessing, heart rate estimation, MI detection, arrhythmia classification, server-side inference, and mobile result delivery within a unified workflow. Rather than using a single multitask end-to-end classifier, the system combines task-specific ML models in one application pipeline for practical ECG interpretation and mobile-health delivery.

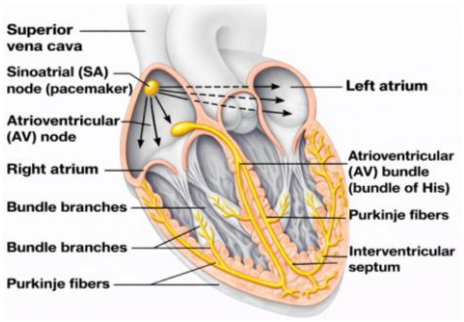


Figure 1. Conduction system of the heart

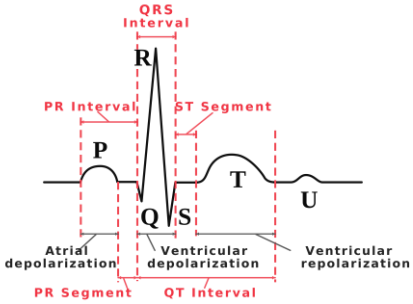


Figure 2. Annotated diagram of key intervals and segments in a typical ECG

2. METHOD

Figure 3 illustrates the overall ECG data-processing and interpretation workflow. The 12-lead ECG signal is transmitted through the mobile application to the server, where biorthogonal and median filtering are applied to reduce noise and baseline wander. The preprocessed signal is subsequently analyzed through two parallel processing paths with distinct functions. The first path focuses on heart rate estimation through R-peak

detection and RR-interval analysis, whereas the second employs task-specific ML models for MI detection and multiclass arrhythmia classification. The resulting heart rate estimates and classification outputs are stored on the server and returned to the mobile application for real-time display and decision support.

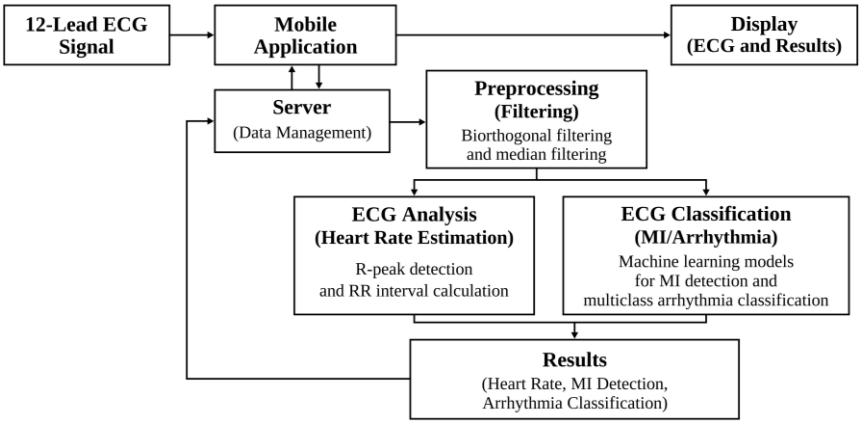


Figure 3. Overall ECG processing workflow illustrating parallel heart rate estimation and MI/arrhythmia classification, followed by mobile delivery of results

2.1. Dataset and evaluation protocol

The proposed framework was developed and evaluated using publicly available 12-lead ECG data from two databases: PTB-XL for arrhythmia classification [21] and the PTB Diagnostic ECG Database [22] for MI detection. After preprocessing and task-specific dataset preparation, each input sample represented a single synchronized row-level 12-lead signal vector extracted from a processed ECG trace, with the class label inherited from the corresponding task label. Thus, the classifiers were trained on row-level signal representations rather than full-record or beat-segment inputs.

Two diagnostic tasks were considered. For MI detection, the labels were organized as a binary problem distinguishing MI from non-MI samples. For arrhythmia analysis, the labels were organized into the target rhythm classes considered in this study. The class distribution of the resulting processed datasets is summarized in Table 1.

Table 1. Class distribution of row-level ECG signal samples used for MI detection and arrhythmia classification

Task	Class	Number of samples (n)	Percentage (%)
MI detection	MI	1,480,000	74.00
	Non-MI	520,000	26.00
	Total	2,000,000	100.00
Arrhythmia classification	SR	377,944	31.16
	AFIB	286,120	23.59
	STACH	158,354	13.06
	SARRH	145,740	12.02
	SBRAD	116,999	9.65
	PACE	56,116	4.63
	SVARR	28,714	2.37
	BIGU	14,778	1.22
	AFLT	14,289	1.18
	SVTAC	5,283	0.44
	PSVT	4,585	0.38
	TRIGU	3,875	0.32
	Total	1,212,797	100.00

For each task, the processed dataset was divided into training and held-out test sets using a random 80/20 split. This split ratio was selected after comparing 60/40, 70/30, 80/20, and 90/10 partitions and identifying 80/20 as the best compromise between training time and predictive performance within this row-level evaluation setup. Model selection was then performed on the training subset using GridSearchCV with stratified 7-fold cross-validation for both diagnostic tasks. To address class imbalance in the arrhythmia

task, oversampling was performed only after the train-test split to prevent information leakage into the held-out test set [23]. All models were implemented in Python, and the same preprocessing, cross-validation, and held-out evaluation pipeline was applied consistently across all compared classifiers.

Final performance was reported on the held-out test set using accuracy, precision, recall, and F1-score, while training performance was reported separately only to describe model fit. In addition, class-wise performance was examined to identify weaker minority-class results, and 95% Wilson confidence intervals were calculated for held-out test accuracy [24]. Because evaluation was performed using row-level random splits of data from the two source databases, the reported results reflect within-dataset row-level generalization and do not establish patient-wise or external clinical generalizability. Patient-wise and external validation are therefore necessary before stronger conclusions about real-world performance can be drawn. This study used only publicly available de-identified ECG data from the PTB Diagnostic ECG Database and PTB-XL, and no new human-subject data were collected.

2.2. Preprocessing

The preprocessing stage begins with the application of a biorthogonal filter to the raw ECG signal, followed by a median filter. The biorthogonal filter is used to reduce unwanted noise, whereas the median filter is applied to correct baseline wander [25], [26].

The filtered signal was then analyzed using the NeuroKit2 ecg_peaks function to identify R peaks for heart rate variability analysis. By using the filtered signal and the sampling rate as inputs, the function identifies beat-to-beat intervals for subsequent analysis. After R-peak detection, the hrv_time function is used to calculate time-domain HRV measures, including HRV_MeanNN, which represents the mean of all normal-to-normal intervals between adjacent QRS complexes associated with sinus rhythm (SR). This value is initially expressed in milliseconds and is converted to seconds by dividing by 1000. The mean heart rate is then calculated by dividing 60 by the mean normal-to-normal interval, as shown in (1):

$$\text{Heart rate (bpm)} = 60/\text{HRV_MeanNN(s)} \quad (1)$$

2.3. Machine learning models

Figure 4 presents the ML workflow adopted for ECG interpretation in the proposed framework. Following preprocessing, the processed 12-lead ECG data were analyzed through two task-specific classification branches integrated within the same system architecture: a MI detection branch and an arrhythmia classification branch. For MI detection, random forest (RF) classifiers using both Gini and entropy criteria were compared with HistGradientBoosting, GradientBoosting, and LightGBM models. For arrhythmia classification, RF, HistGradientBoosting, and LightGBM classifiers were evaluated. Hyperparameter tuning was conducted on the training subset using GridSearchCV with stratified 7-fold cross-validation for both MI detection and arrhythmia classification.

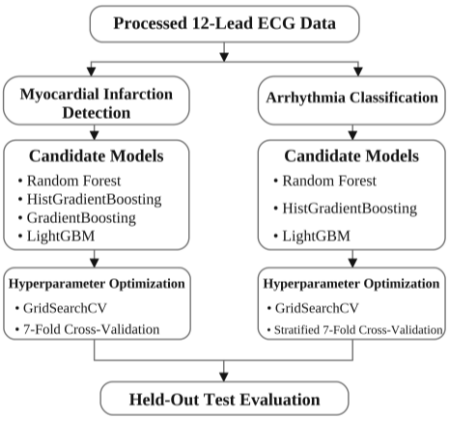


Figure 4. ML workflow for MI detection and arrhythmia classification

The best-performing models were subsequently assessed on the independent held-out test set under the row-level evaluation protocol described in subsection 2.1. The hyperparameter settings explored for the evaluated models are summarized in Tables 2–5. Model performance was evaluated using standard classification metrics, including accuracy, precision, recall, and F1-score [23].

Table 2. RF models with entropy criterion evaluated for MI detection

Trial	Criterion	Number of estimators	Max depth	Min samples split	Min samples leaf
1	Entropy	45	20	2	1
2	Entropy	45	30	2	1
3	Entropy	45	45	5	2
4	Entropy	45	45	2	1
5	Entropy	60	30	2	1

Table 3. RF models with Gini criterion evaluated for MI detection

Trial	Criterion	Number of estimators	Max depth
1	Gini	45	45
2	Gini	60	45
3	Gini	100	45
4	Gini	150	45
5	Gini	200	45

Table 4. Boosting-based models evaluated for MI detection

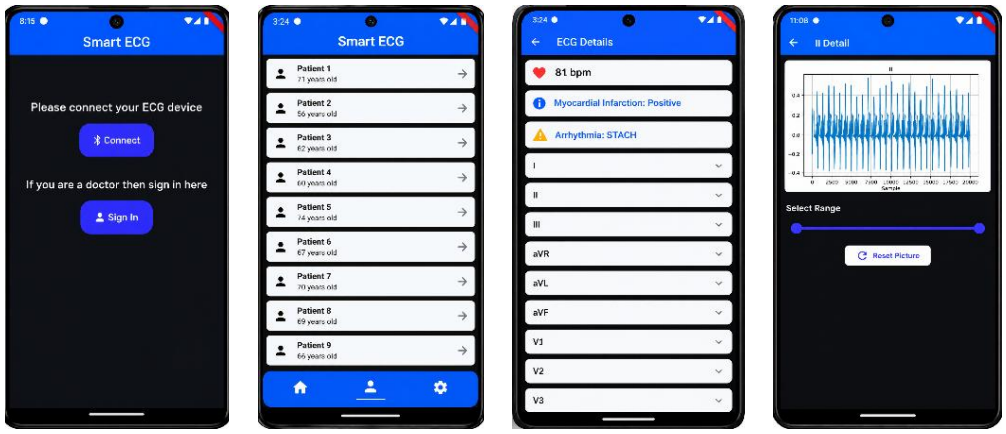
Classifier	Learning rate	L2 regularization	Max depth	Min leaf / child samples	Max leaf nodes	Max bins
HistGradientBoosting	0.1	10	30	10	63	255
GradientBoosting	1	-	10	10	63	-
LightGBM	1	-	10	20	-	255

Table 5. Classifiers using different parameters for Arrhythmia classification

Classifier	Learning rate	Max depth	Max iterations	Min leaf/child samples	Criterion	Number of estimators
HistGradientBoosting	0.1	20	100	20	–	–
RF	–	45	–	–	Gini	200
RF	–	45	–	–	Entropy	200
LightGBM	0.1	20	–	20	–	200

2.4. Mobile application

The mobile application was developed using Flutter for cross-platform deployment, whereas Flask was used on the backend to connect the application to the server through application programming interfaces (APIs). This architecture enables ECG signal transfer, server-side analysis, and delivery of diagnostic outputs to the user interface. Figure 5 illustrates the main interfaces of the developed mobile application. Figure 5(a) shows the ECG device connection and user sign-in interface, Figure 5(b) displays the patient selection list, Figure 5(c) presents the heart rate estimate and the MI detection and arrhythmia classification results, and Figure 5(d) illustrates the visualization of a selected ECG lead with an adjustable signal display range. These interfaces demonstrate functional integration of ECG acquisition, server-side inference, and mobile result delivery. However, latency, communication delay, and deployment robustness were not quantified in the present study and should be evaluated in future system-level testing.



(a) (b) (c) (d)

Figure 5. Mobile application interface: (a) connection and sign-in, (b) patient list, (c) diagnostic output, and (d) ECG lead visualization

3. RESULTS AND DISCUSSION

The preprocessing pipeline improved ECG signal quality in two stages. First, the biorthogonal filter reduced high-frequency noise while preserving clinically relevant waveform morphology, as illustrated in Figure 6. Second, the median filter reduced low-frequency baseline wander without distorting the overall ECG shape, as shown in Figure 7. Together, these steps improved the clarity of the 12-lead ECG signals, thereby reducing the likelihood that noise or baseline drift would obscure diagnostically relevant patterns required for MI detection and arrhythmia classification.

The filtered signal was then analyzed using the NeuroKit2 ecg_peaks function to identify R peaks for heart rate variability analysis. As shown in Figure 8, the peaks detected were well aligned with the ECG waveform, supporting reliable beat-to-beat interval estimation. Figure 9 shows that the R-R intervals were concentrated around 730 ms and 745 ms, corresponding to an estimated mean heart rate of 81 beats per minute based on the HRV_MeanNN metric. These findings indicate that the preprocessing and peak-detection pipeline preserved sufficient temporal information for practical heart rate estimation and real-time physiological monitoring.

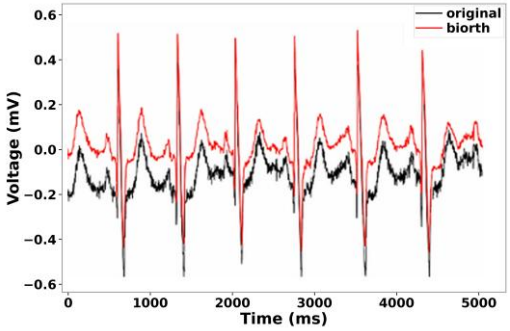


Figure 6. Original and filtered ECG signals using biorthogonal filtering

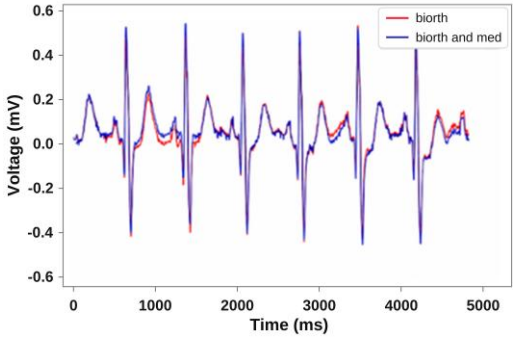


Figure 7. ECG signal after biorthogonal filtering and after subsequent median filtering

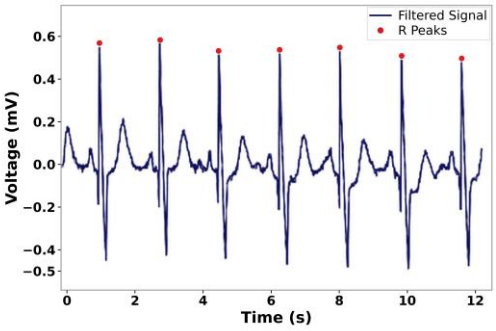


Figure 8. Visualization of R-peak detection in the filtered ECG signal

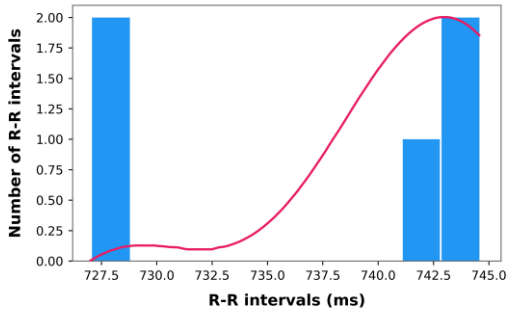


Figure 9. Histogram and curve of R-R interval distribution indicating heart rate variability

For MI detection, the RF model achieved the highest held-out test accuracy (96.89%) using the Gini criterion with max_depth=45 and n_estimators=200. Figure 10 shows the confusion matrix of the final model. In contrast, HistGradientBoosting produced the lowest accuracy (83.51%), whereas GradientBoosting and LightGBM achieved 87.18% and 89.21%, respectively, as summarized in Table 6. Table 7 reports the summary evaluation metrics derived from the held-out test predictions. The superior performance of the RF model suggests that the selected preprocessing and row-level signal representation were better matched to this binary classification task. By contrast, the weaker performance of the boosting-based models may indicate greater sensitivity to the feature representation and parameter settings used in this study. Based on 387,547 correct predictions out of 400,000 test samples, the 95% Wilson confidence interval for MI detection accuracy was 96.83%–96.94%.

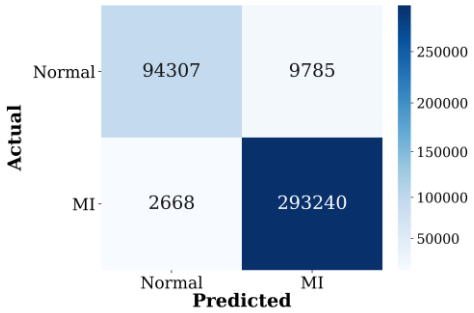


Figure 10. Confusion matrix of the held-out test results for MI detection using the RF model with the Gini criterion

Table 6. Held-out test accuracy comparison of evaluated classifiers for MI detection

Classifier	Held-out test accuracy (%)	Best parameters
RF	96.89	criterion=gini; max_depth=45; n_estimators=200
HistGradientBoosting	83.51	l2_regularization=10; learning_rate=0.1; max_bins=255; max_depth=30; max_iter=100; max_leaf_nodes=63; min_samples_leaf=10
GradientBoosting	87.18	learning_rate=1; max_depth=10; max_leaf_nodes=63; min_samples_leaf=10; n_estimators=100; subsample=0.5
LightGBM	89.21	learning_rate=1; max_bin=255; max_depth=10; min_child_samples=20; n_estimators=200; num_leaves=50; reg_lambda=1.0

Table 7. Summary evaluation metrics for MI detection derived from the held-out test set

Metric	Value (%)
Accuracy	96.887
Macro-averaged precision	97.010
Macro-averaged recall	94.849
Macro-averaged F1-score	95.864

For arrhythmia classification, the RF model with the Gini criterion achieved the best held-out test accuracy (89.59%), followed by the entropy-based RF model (88.91%), whereas LightGBM and HistGradientBoosting achieved lower accuracies of 49.80% and 36.26%, respectively, as summarized in Table 8. The selected Gini-based RF model achieved 97.0% accuracy on the oversampled training subset and 89.59% on the held-out test set, indicating reduced generalization relative to model fit on the training data. Table 9 summarizes the held-out test evaluation metrics and Figure 11 shows the corresponding confusion matrix. The corresponding 95% Wilson confidence interval for held-out test accuracy was 89.46%–89.71%. The lower macro-averaged scores relative to the weighted-averaged scores indicate that minority rhythm classes remained more challenging.

Table 8. Held-out test accuracy comparison of evaluated classifiers for arrhythmia classification

Classifier	Held-out test accuracy (%)	Best parameters
RF (Gini)	89.59	criterion=gini; max_depth=45; n_estimators=200
RF (Entropy)	88.91	criterion=entropy; max_depth=45; n_estimators=200
HistGradientBoosting	36.26	learning_rate=0.1; max_depth=20; max_iter=100; min_samples_leaf=20
LightGBM	49.80	learning_rate=0.1; max_bin=255; max_depth=20; min_child_samples=20; n_estimators=200; num_leaves=50; reg_lambda=1.0

Table 9. Summary evaluation metrics for arrhythmia classification derived from the held-out test set

Metric	Value (%)
Accuracy	89.585
Macro-averaged precision	77.278
Macro-averaged recall	74.415
Macro-averaged F1-score	75.752
Weighted-averaged precision	89.667
Weighted-averaged recall	89.585
Weighted-averaged F1-score	89.543

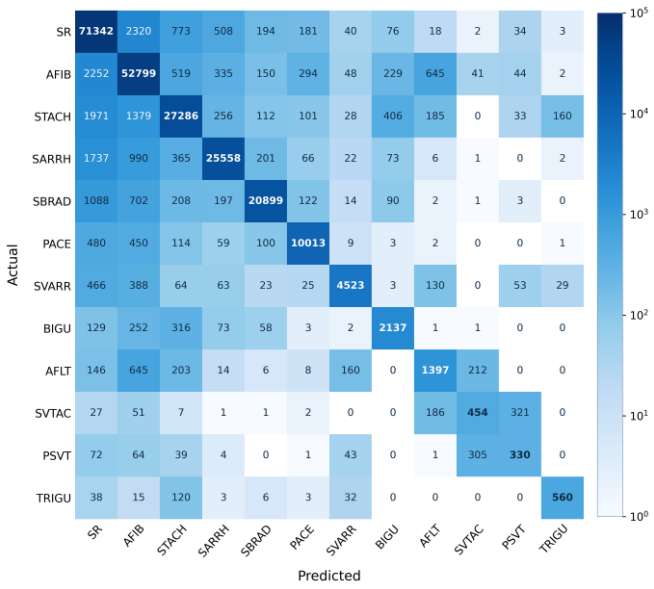


Figure 11. Confusion matrix of the held-out test results for arrhythmia classification using the RF model with the Gini criterion

Class-wise results on the held-out test set were weaker for minority arrhythmia classes, particularly SVTAC and paroxysmal supraventricular tachycardia (PSVT), which had lower precision, recall, and F1-scores than dominant classes such as SR and AFIB, as shown in Table 10. This class imbalance explains why overall accuracy should be interpreted together with class-wise and macro-averaged performance. The weaker performance in minority classes such as SVTAC and PSVT is likely related not only to their limited sample sizes, but also to greater morphological overlap with other supraventricular rhythm categories and the reduced diversity of training examples available for these classes. In contrast, dominant classes such as SR and AFIB were represented by substantially larger numbers of samples, allowing the model to learn more stable class boundaries. These findings indicate that future performance gains will likely depend not only on classifier choice, but also on improved class balancing, broader representation of rare rhythms, and validation under more clinically heterogeneous conditions.

Table 10. Class-wise performance for arrhythmia classification on the held-out test set

Arrhythmia type	Precision (%)	Recall (%)	F1-score (%)	Support (n)
SR	89.459	94.504	91.912	75,491
AFIB	87.918	92.052	89.937	57,358
STACH	90.911	85.490	88.117	31,917
SARRH	94.411	88.067	91.129	29,021
SBRAD	96.087	89.595	92.728	23,326
PACE	92.550	89.155	90.821	11,231
SVARR	91.912	78.429	84.637	5,767
BIGU	70.832	71.904	71.364	2,972
AFLT	54.295	50.054	52.088	2,791
SVTAC	44.641	43.238	43.928	1,050
PSVT	40.342	38.417	39.356	859
TRIGU	73.976	72.072	73.012	777

The classification labels are defined as follows: STACH: sinus tachycardia, SARRH: sinus arrhythmia, SBRAD: sinus bradycardia, PACE: paced rhythm, SVARR: supraventricular arrhythmia, BIGU: bigeminy, AFLT: atrial flutter, and TRIGU: trigeminy.

Direct comparison with previous studies is limited because reported performance depends strongly on differences in datasets, label definitions, input representations, preprocessing strategies, class structure, and validation protocols [13], [16]–[19]. Table 11 is therefore provided as a contextual comparison rather than as a controlled same-protocol benchmark. The main value of this work lies in its end-to-end engineering integration of MI detection, arrhythmia classification, and mobile result delivery within a single workflow.

Table 11. Comparison with representative recent studies

Study	Task and data	Model	Main result
Śmigiel *et al.* [16]	PTB-XL ECG classification (2, 5, and 20 classes)	CNN+entropy features	89.2%, 76.5%, and 69.8% accuracy
Qu *et al.* [17]	PTB MI	Interpretable shapelet-based deep model	94.11% accuracy, 94.97% sensitivity, and 90.98% specificity
Sattar *et al.* [18]	Digitized ECG arrhythmia classification (CPEIC dataset)	CNN	91.8% accuracy; suitable for direct real-time monitoring
Baca and Valdivia [19]	Wearable-oriented arrhythmia study and MIT-BIH validation	1D CNN	99.57% multiclass accuracy and 68.48 MFLOPs
Present work	Unified MI+arrhythmia workflow using PTB Diagnostic and PTB-XL ECG data	RF+IoT-enabled mobile delivery	96.89% MI held-out row-level test accuracy and 89.59% arrhythmia held-out row-level test accuracy

3.1. Limitations and practical implications

This study has several limitations. The evaluation used random row-level splits of ECG data from the PTB Diagnostic ECG Database and PTB-XL, so the results reflect within-dataset row-level generalization rather than patient-wise or external clinical performance. The arrhythmia task also remained affected by class imbalance, with weaker performance in minority classes such as SVTAC and PSVT. In addition, although the framework demonstrated mobile-connected inference, system-level measures such as latency, communication delay, robustness, and computational cost were not benchmarked. The proposed framework should therefore be interpreted as a decision-support prototype. Future work should focus on patient-wise validation, external multi-center testing, deployment-oriented system evaluation, and the investigation of explainable artificial intelligence (AI) approaches that can highlight decision-relevant ECG patterns to improve transparency, support clinical trust, and facilitate deployment in real-world decision-support settings.

4. CONCLUSION

This study presented a unified mobile framework for ECG-based MI detection and arrhythmia classification. The main contribution lies in integrating ECG preprocessing, task-specific ML inference, and mobile result delivery within a single workflow for practical ECG interpretation and remote follow-up. Using data from the PTB Diagnostic ECG Database for MI detection and PTB-XL for arrhythmia classification, the best RF model achieved 96.89% accuracy for MI detection, while the selected RF model achieved 89.59% accuracy for arrhythmia classification on the held-out test set. These findings support the potential of the proposed framework as a practical mobile decision-support system for ECG interpretation and remote follow-up. Because evaluation was performed using row-level random splits rather than patient-disjoint validation, the reported results should be interpreted as within-dataset decision-support performance rather than patient-level clinical performance. Further validation should therefore prioritize patient-disjoint and external testing, improved robustness for minority rhythm classes, and system-level benchmarking of latency and deployment robustness in wearable and remote-monitoring settings.

ACKNOWLEDGMENTS

The authors have no additional acknowledgments to declare.

FUNDING INFORMATION

This research was supported by the following research grant or contract funding sources: Seed Grant No. SAMS 03/2023 from the German Jordanian University (Decision No. 2023/15/344), a grant from Aeon Medical Supplies Company, and the Scientific Research and Innovation Support Fund (SRISF), Jordan (Project No. SE-MPH/4/2024). The funding bodies had no role in study design, data processing, model development, result interpretation, manuscript preparation, or the decision to publish.

AUTHOR CONTRIBUTIONS STATEMENT

This journal uses the Contributor Roles Taxonomy (CRediT) to recognize individual author contributions, reduce authorship disputes, and facilitate collaboration.

Name of Author	C	M	So	Va	Fo	I	R	D	O	E	Vi	Su	P	Fu
Sameer Ahmad Hasan	✓	✓		✓	✓	✓		✓	✓	✓		✓	✓	
Samer Alabed		✓		✓					✓	✓				✓
Talal Ayyoub		✓	✓			✓		✓	✓		✓			
Abdullah Shahin		✓	✓	✓					✓		✓			

C : **C**onceptualization
M : **M**ethodology
So : **So**ftware
Va : **Va**lidation
Fo : **Fo**rmal analysis
I : **I**nvestigation
R : **R**esources
D : **D**ata Curation
O : Writing - **O**riginal Draft
E : Writing - Review & **E**diting
Vi : **Vi**sualization
Su : **Su**pervision
P : **P**roject administration
Fu : **Fu**nding acquisition

CONFLICT OF INTEREST STATEMENT

The authors declare that they have no known competing financial, personal, or professional interests that could have appeared to influence the work reported in this paper.

DATA AVAILABILITY

The ECG data used in this study were obtained from two publicly available databases hosted on PhysioNet: PTB-XL [21] and the PTB Diagnostic ECG Database [22]. Derived data supporting the findings of this study are available from the corresponding author upon reasonable request.

REFERENCES

[1] "Cardiovascular diseases (CVDs)," *World Health Organization News Room*, 2021. https://www.who.int/news-room/fact-sheets/detail/cardiovascular-diseases-(cvds). (Accessed Aug. 01, 2023).

[2] "Strengthening the prevention and management of cardiovascular disease risk factors through primary health care in Jordan," *World Health Organization*, 2020. https://www.who.int/about/accountability/results/who-results-report-2020-mtr/country-story/2021/jordan. (Accessed Aug. 02, 2024).

[3] J. A. Shah *et al.*, "Incidence of cardiac arrhythmias in acute myocardial infarction patients undergoing primary percutaneous coronary intervention and associated outcomes during the first 24 hours," *Cureus*, vol. 13, no. 1, Jan. 2021, doi: 10.7759/cureus.12599.

[4] D. S. Park and G. I. Fishman, "The cardiac conduction system: development, function and therapeutic targets," *Nature Reviews Cardiology*, vol. 23, no. 5, pp. 303–323, May 2026, doi: 10.1038/s41569-025-01227-x.

[5] Z. Kotsialou, N. Makris, and S. Gall, "Fundamentals of the electrocardiogram and common cardiac arrhythmias," *Anaesthesia & Intensive Care Medicine*, vol. 25, no. 3, pp. 219–222, Mar. 2024, doi: 10.1016/j.mpaic.2023.11.014.

[6] A. Lashrf and A. Salim, "Interpretation of electrocardiogram," *InnovAiT: Education and inspiration for general practice*, vol. 17, no. 11–12, pp. 488–494, Nov. 2024, doi: 10.1177/17557380241282287.

[7] S. Y. Kim, J.-P. Lee, W.-R. Shin, I.-H. Oh, J.-Y. Ahn, and Y.-H. Kim, "Cardiac biomarkers and detection methods for myocardial infarction," *Molecular & Cellular Toxicology*, vol. 18, no. 4, pp. 443–455, Oct. 2022, doi: 10.1007/s13273-022-00287-1.

[8] J. Kingma, C. Simard, and B. Drolet, "Overview of cardiac arrhythmias and treatment strategies," *Pharmaceuticals*, vol. 16, no. 6, Jun. 2023, doi: 10.3390/ph16060844.

[9] D. S. Desai and S. Hajouli, "Arrhythmias," *StatPearls*, 2023. https://www.ncbi.nlm.nih.gov/books/NBK558923/. (Accessed Aug. 02, 2024).

[10] W. Li, "Wavelets for electrocardiogram: Overview and taxonomy," *IEEE Access*, vol. 7, pp. 25627–25649, 2019, doi: 10.1109/ACCESS.2018.2877793.

[11] H. Y. Mir and O. Singh, "ECG denoising and feature extraction techniques – a review," *Journal of Medical Engineering & Technology*, vol. 45, no. 8, pp. 672–684, Nov. 2021, doi: 10.1080/03091902.2021.1955032.

[12] G. Petmezas *et al.*, "State-of-the-art deep learning methods on electrocardiogram data: Systematic review," *JMIR Medical Informatics*, vol. 10, no. 8, Aug. 2022, doi: 10.2196/38454.

[13] M. Sraitih, Y. Jabrane, and A. H. El Hassani, "A robustness evaluation of machine learning algorithms for ECG myocardial infarction detection," *Journal of Clinical Medicine*, vol. 11, no. 17, Aug. 2022, doi: 10.3390/jcm11174935.

[14] E. Radwa, H. Ridha, and B. Faycal, "Deep learning-based approaches for myocardial infarction detection: A comprehensive review recent advances and emerging challenges," *Medicine in Novel Technology and Devices*, vol. 23, Sep. 2024, doi: 10.1016/j.medntd.2024.100322.

[15] A. Darmawahyuni *et al.*, "An improved electrocardiogram arrhythmia classification performance with feature optimization," *BMC Medical Informatics and Decision Making*, vol. 24, no. 1, Dec. 2024, doi: 10.1186/s12911-024-02822-7.

[16] S. Śmigiel, K. Pałczyński, and D. Ledziński, "ECG signal classification using deep learning techniques based on the PTB-XL dataset," *Entropy*, vol. 23, no. 9, Aug. 2021, doi: 10.3390/e23091121.

[17] J. Qu *et al.*, "An interpretable shapelets-based method for myocardial infarction detection using dynamic learning and deep learning," *Physiological Measurement*, vol. 45, no. 3, Mar. 2024, doi: 10.1088/1361-6579/ad2217.

[18] S. Sattar *et al.*, "Cardiac Arrhythmia Classification Using Advanced Deep Learning Techniques on Digitized ECG Datasets," *Sensors*, vol. 24, no. 8, Apr. 2024, doi: 10.3390/s24082484.

[19] H. A. H. Baca and F. de L. P. Valdivia, "Efficient deep learning-based arrhythmia detection using smartwatch ECG electrocardiograms," *Sensors*, vol. 25, no. 17, Aug. 2025, doi: 10.3390/s25175244.

[20] C. Han, J. Sun, Y. Bian, W. Que, and L. Shi, "Automated detection and localization of myocardial infarction with interpretability analysis based on deep learning," *IEEE Transactions on Instrumentation and Measurement*, vol. 72, pp. 1–12, 2023, doi: 10.1109/TIM.2023.3258521.

[21] P. Wagner *et al.*, "PTB-XL, a large publicly available electrocardiography dataset," *Scientific Data*, vol. 7, no. 1, May 2020, doi: 10.1038/s41597-020-0495-6.

[22] R. Bousseljot, D. Kreiseler, and A. Schnabel, "Nutzung der EKG-Signaldatenbank CARDIODAT der PTB über das Internet," *Biomedizinische Technik*, vol. 40, pp. 317–318, 1995, doi: 10.1515/bmte.1995.40.s1.317.
[23] M. Salmi, D. Atif, D. Oliva, A. Abraham, and S. Ventura, "Handling imbalanced medical datasets: review of a decade of research," *Artificial Intelligence Review*, vol. 57, no. 10, Sep. 2024, doi: 10.1007/s10462-024-10884-2.
[24] O. Rainio, J. Teuho, and R. Klén, "Evaluation metrics and statistical tests for machine learning," *Scientific Reports*, vol. 14, no. 1, Mar. 2024, doi: 10.1038/s41598-024-56706-x.
[25] Y. Jia *et al.*, "Preprocessing and denoising techniques for electrocardiography and magnetocardiography: A review," *Bioengineering*, vol. 11, no. 11, Nov. 2024, doi: 10.3390/bioengineering11111109.
[26] H. Zhao, T. Li, J. Yang, and C. Pang, "An error-bounded median filter for correcting ECG baseline wander," *Health Information Science and Systems*, vol. 11, no. 1, Sep. 2023, doi: 10.1007/s13755-023-00235-w.

BIOGRAPHIES OF AUTHORS



Sameer Ahmad Hasan is an assistant professor of Biomedical Engineering at the German Jordanian University, Amman, Jordan. He received his Ph.D. in Biomedical Engineering from Northumbria University, United Kingdom, and has more than 20 years of experience across academia, research, and industry. His research focuses on biomedical instrumentation, advanced sensor systems, medical signal and image processing, and AI-based healthcare technologies. His research has covered surface acoustic wave sensor development, contactless vital-sign monitoring, AI-assisted medical diagnostics, and IoT-enabled healthcare systems. He has led and supervised projects in seizure detection, diabetic foot assessment, impedance-based gesture recognition, biosignal analysis, and smart biosensing applications. His broader research interests include interdisciplinary and translational innovation linking engineering technologies with clinical and healthcare needs. He can be contacted at email: sameer.hasan@gju.edu.jo.



Samer Alabed is a professor of Electrical and Biomedical Engineering at the German Jordanian University (GJU), a Strategic Academic Leader, and an expert in signal processing, internet of things (IoT), and AI. Throughout his tenure at GJU, he has held several key academic and administrative leadership positions, including head of Department of Biomedical Engineering, Exchange Coordinator for the German Year Program, Director of the Department of Accreditation and Quality Assurance, and Director of the Department of E-Learning and Academic Performance Improvement. Prior to joining GJU, he served as an associate professor at the American University of the Middle East, Kuwait, from 2015 to 2022. He earned his Ph.D. in Electrical Engineering and Information Technology from TU-Darmstadt, Germany. From 2008 to 2015, he was also affiliated with TU Darmstadt, where he contributed to academic and research activities in electrical engineering, with a focus on digital signal processing and related technologies. He can be contacted at email: samer.alabed@gju.edu.jo.



Talal Ayyoub is a Biomedical Engineering graduate of the German Jordanian University, Amman, Jordan. His academic and professional interests include biomedical signal processing, AI, and medical device development. During his studies, he completed an exchange semester at Fulda University of Applied Sciences, Germany, where he broadened his technical background in biomedical systems and applied engineering practice. His graduation project focused on the development of a smart electrocardiogram system integrating AI-based arrhythmia and myocardial infarction detection for remote patient monitoring. He also completed an internship in product and quality management, where he gained practical experience in technical documentation, compliance procedures, and internal audits within the medical device sector. His broader interests include digital health solutions, intelligent diagnostic support, and translational biomedical engineering applications. He can be contacted at email: t.ayyoub@gju.edu.jo.



Abdullah Shahin is a Biomedical Engineering graduate of the German Jordanian University, Amman, Jordan. His interests include embedded systems, biomedical signal processing, and ML methods for medical diagnosis and monitoring. During his academic training, he completed a research semester at the Department of Measurement and Sensor Technology, Chemnitz University of Technology, Germany, where he worked on embedded battery diagnostic systems and signal acquisition. His graduation project focused on myocardial infarction detection and arrhythmia classification using electrocardiogram data and machine learning models within a connected mobile-health framework. He also completed an internship at Stockert GmbH in Freiburg, Germany, where he contributed to product development and validation activities related to pulsed field ablation systems. His broader interests include intelligent diagnostic platforms, physiological monitoring systems, and practical biomedical engineering innovation. He can be contacted at email: a.shahin1@gju.edu.jo.